Hardware Realization of Participants in an Energy Packet-based Power Grid

1st Dominik Schulz
Institute of Electrical Engineering (ETI)
Karlsruhe Institute of Technology (KIT)
Karlsruhe, Germany
dominik.schulz@kit.edu

2nd Klemens Schneider
Institute of Telematics (TM)
Karlsruhe Institute of Technology (KIT)
Karlsruhe, Germany
klemens.schneider@kit.edu

3rd Marcel Weßbecher
Institute for Automation and Applied Informatics (IAI)
Karlsruhe Institute of Technology (KIT)
Karlsruhe, Germany
marcel.wessbecher@kit.edu

4th Veit Hagenmeyer
Institute for Automation and Applied Informatics (IAI)
Karlsruhe Institute of Technology (KIT)
Karlsruhe, Germany
veit.hagenmeyer@kit.edu

5th Martina Zitterbart
Institute of Telematics (TM)
Karlsruhe Institute of Technology (KIT)
Karlsruhe, Germany
martina.zitterbart@kit.edu

6th Marc Hiller
Institute of Electrical Engineering (ETI)
Karlsruhe Institute of Technology (KIT)
Karlsruhe, Germany
marc.hiller@kit.edu

***Abstract*—The many changes and challenges faced by power grids have generated scientific interest in possible architectures for the next-generation power grid. An emerging approach is the energy packet grid (EP grid), a new paradigm for the power grid that is inspired by selected Internet design principles, in which grid participants exchange energy packets (EPs). We propose a hardware realization of participants in such an EP grid. This realization enables a comprehensive verification of EP concepts and protocols. The present paper discusses the necessary power electronic components together with a signal processing and control architecture. Laboratory measurements show first energy packet transfers and validate the presented concept.**

***Index Terms*—energy packets, energy system transformation, energy packet device, microgrids, power electronic grids**

I. Introduction

Power grids around the world face fundamental changes due to the need to switch from fossil fuels to exclusively renewable energy sources. As the share of power generation provided by distributed energy resources rises, the structure of the grid shifts to a more decentralized power supply. This comes with new challenges, as the power lines and grid equipment installed today were not designed to support the power flows arising from distributed generation [1], [2]. The strains on the power grid are further exacerbated by the electrification of mobility and heat [3]. Additionally, the availability of these new energy sources is no longer controllable. Therefore, their variable generation must now be matched by flexible loads and coordinated use of storage options. Centralized control and grid management face prohibitively high complexity and inflexibility due to an increasing amount of measurement data and possible control signals, together with their required communication. The microgrid paradigm [4], [5] and more advanced concepts including multi-microgrids [6], web of cells and fractal grids [7] all envision a decentralized and autonomous control of participants, which can then be treated as a single aggregated entity by higher control layers. While these approaches mitigate the control complexity of the future grid, they offer no clear solution on the scalable coordination of available energy supply and flexible demand, together with the management of shared and limited resources, especially line capacities, transformer ratings and energy storage levels. Similar challenges were overcome in communication networks by employing packet switching. An emerging approach therefore consists of organizing the power flows through the grid into discrete energy packets. This concept was first proposed in [8] and later further discussed in particular in [9]–[11]. In these works, energy packet transfers are accomplished by interconnecting capacitors charged with DC voltage, but there is no control over the transmitted power, and exclusive line usage between participants is required.

This work was supported by the KIT Future Fields Stage 2 funding program

Furthermore, the energy internet and related designs as successors to the smart grid are further concepts to solve the challenges of future power grids [12]–[19]. While they share similarities with the proposed energy packet (EP) grid, they do not necessarily employ discrete energy packets or remain on a higher system level. Recently, packetized energy management inspired by communication theory concepts was applied to thermostats and electric vehicle (EV) charging schemes [20]–[23]. These works demonstrate the advantage of efficient grid resource utilization if a central coordinator can authorize loads to turn on during discrete time steps. The EP grid proposed by the authors in [24] constitutes a more extensive approach, in which conceivably all power flows in the grid consist of energy packets with specified power levels. This way, the local power balance can be maintained by design while also respecting grid equipment limits. The present paper builds on the envisioned architecture introduced in [24] and will detail the design of a hardware realization of participants in an EP grid. These can then be used to form an experimental EP grid and to show the feasibility of such EP transfers.

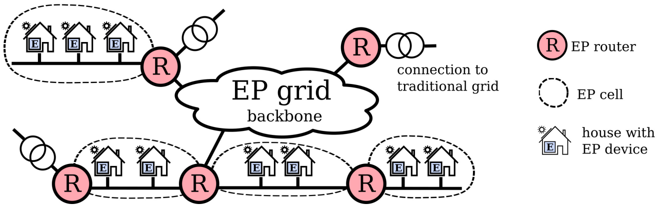

Fig. 1. Example EP grid consisting of several EP cells

II. Energy packet-based power grid

The EP grid is inspired by the Internet as a network of networks [24]. Accordingly, the power grid is partitioned into smaller subnetworks called EP cells, which are separate electric grids. These self-organized EP cells can flexibly be configured to operate with DC or asynchronous AC voltage independent of adjacent EP cells. This layered design principle shown in Fig. 1 allows for simplified adoption and integration of existing infrastructure. Participants within an EP cell are named EP devices. They cooperatively control the currents and the power balance of the EP cell and at least one EP device is tasked with maintaining the EP cell voltage. To this end, each EP device is equipped with power electronics and communication interfaces. Each power electronic interface must take an electric role. It can either be a voltage controller or a current controller in the EP cell [24]. If the EP device contains more than one power electronic interface, it can also serve as an EP router linking neighboring EP cells. An EP router can assume multiple roles, for example, it can be a voltage controller in one EP cell and a current controller in another EP cell.

EP devices transfer energy packets to each other according to present and projected supply and demand. This is accomplished by an EP transfer protocol, e. g. the Simple Energy Packet Transfer protocol (SEPT) [24]. SEPT enables EP devices that reside within the same EP cell to negotiate the parameters of an EP transfer. In the current implementation, these include the total packet energy W_{EP}, ramping times t_{r} and the stationary power level P_{EP}. Power curves for an example EP transfer are shown in Fig. 2, with positive power denoting a power flow out of the EP grid. The total energy exchanged using the energy packet is defined by the time integral of the power curve, thus $W_{\mathrm{EP}} = \int_{t_0}^{t_0+t_{\mathrm{EP}}} p(\tau)d\tau$.

Due to the communication latency between the two EP devices, the power curve of the second EP device is delayed by t_{del}. In order to satisfy the power equilibrium $\sum_i p_i = 0$ in the EP grid, the negative sum of the two power curves $p_\Delta = -(p_1+p_2)$ needs to be supplied or consumed by another EP device with according energy reserves, for example, the grid voltage controller. One reason the power packet is chosen to be of a trapezoidal shape is to reduce the compensation power demand caused by communication delays. The ramping phases at the start and end of each energy packet lower the peak compensation power.

SEPT also requires all EP transfers to be registered at the Line Manager. The Line Manager is a software component

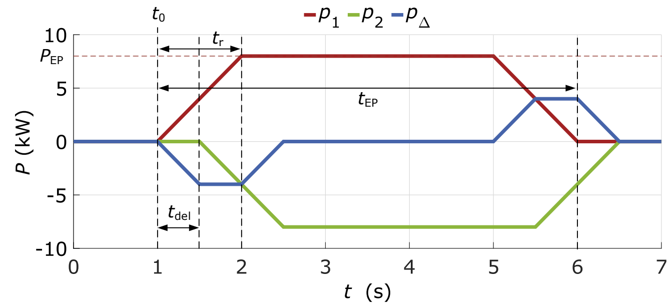

Fig. 2. Ideal power curves for an example EP transfer with communication latency

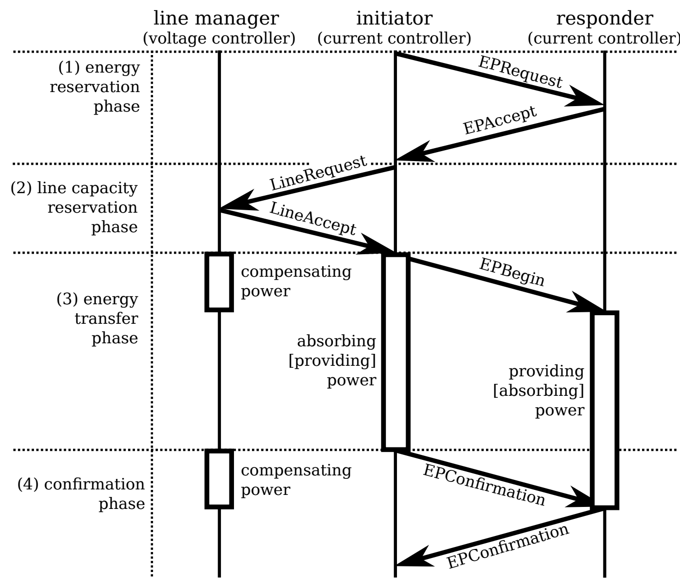

Fig. 3. Messages and phases of an EP transfer between two current-controlled EP devices according to SEPT [24]

that approves requests for EP transfers and thus ensures that the power line transmission limits are not exceeded. This way, the known advantages of packet switching in communication networks such as improved line utilization can be exploited in the EP grid. The phases and exchanged messages for EP transfers between two EP devices acting as current controllers are shown in Fig. 3.

III. Realization of participants

Based on the previous high-level description of participants in an EP-based grid, in this section, we describe the hardware implementation of such EP devices.

A. General Architecture and Signal Processing

The general hardware architecture and associated system interfaces are shown in Fig. 4. Each realized participant includes a standard personal computer (PC), a system on a chip (SoC), local control units (LCUs) and power electronics. The SEPT application runs on the PC, which contains two Ethernet network interfaces. The first enables communication with other EP devices within the laboratory network, while

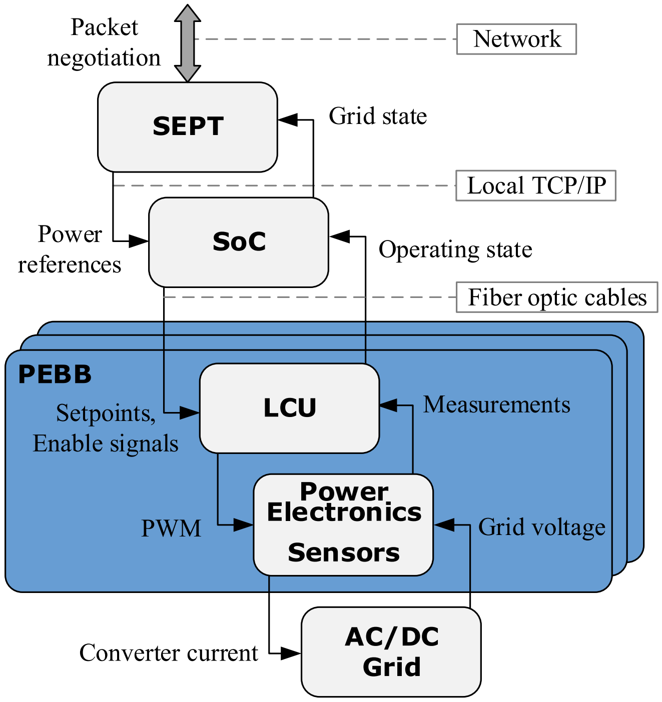

Fig. 4. Architecture and system interfaces of the realized energy packet device

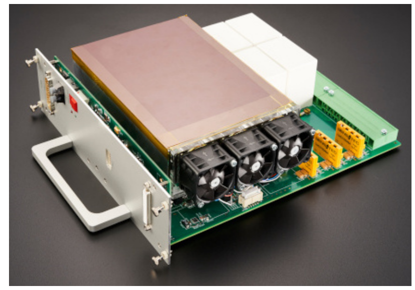

Fig. 5. Three-phase AC/DC converter as power electronic building block (PEBB) with mounted local control unit

TABLE I
HARDWARE PARAMETERS

Symbol	Parameter	Value	
	AC side		
		SiC	IGBT
L_{grid}	Grid-side inductance	50 µH	150 µH
$L_{\mathrm{converter}}$	Converter-side inductance	100 µH	1 mH
C_{LCL}	LCL capacitance (delta)	4.7 µF	6 µF
L_{CM}	Common-mode inductance	10.5 mH	10.5 mH
f_{sw}	Switching frequency	50 kHz	10 kHz
	DC side		
n_{xfmr}	DAB transformer turns ratio	1 : 1	
$f_{\mathrm{sw,DAB}}$	DAB switching frequency	50 kHz	
$L_{\mathrm{DC/DC}}$	DC/DC converter inductance	300 µH	
$f_{\mathrm{sw,DC/DC}}$	DC/DC switching frequency	50 kHz	
C_{DC1}	Total DC link 1 capacitance	1.4 mF	
C_{DC2}	Total DC link 2 capacitance	1.4 mF	
C_{DC2}	Total DC link 3 capacitance	1.4 mF	

the second one is used to interact with the SoC. This SoC constitutes the core of the signal-processing architecture and consists of two ARM cores together with an FPGA and various extension cards. It is described in detail in [25]. In the SoC, the power references defined by the SEPT application are translated into corresponding current or voltage setpoints for the underlying power electronics. At the same time, this SoC system is responsible for the global coordination, which includes specified enabling sequences, contactor switching, limit monitoring and error handling. The resulting setpoints are sent over fiber optic cables to the individual power electronic building blocks (PEBBs), which in turn each consist of an LCU and associated power electronics and sensors. These LCUs are based on Artix-7 FPGAs, which implement the required control algorithms and modulation for the associated power electronics. This way, a modular structure is achieved, where specific control implementation details are encapsulated in the PEBB. Additionally, the LCUs reduce the computational effort on the central SoC and minimize communication delays for the control loops as a result of their physical proximity to the sensors and semiconductor switches. Fig. 5 shows an example of a PEBB utilized for the hardware realization.

B. Hardware Topology

The topology of the power electronics hardware is shown in Fig. 6. It contains three-phase AC terminals on either end. The first set of terminals connects an AC grid to an IGBT active front-end (AFE) using an LCL filter and common-mode (CM) chokes. Its DC link is connected to a dual active bridge (DAB). The secondary DC link of the DAB is connected to an optional interleaved synchronous buck converter stage, feeding a third DC link. This also forms the DC side of a second AFE based on SiC MOSFETs, which is connected to the second AC grid via another LCL filter.

The four converter stages indicated in Fig. 6 consist of previously developed, modular PEBBs with a power rating of 30 kW, one of which is shown in Fig. 5. All three DC links can be contacted over a connection panel, such that the EP device may form part of both an AC and DC grid. The DAB provides galvanic isolation, while the bidirectional DC/DC converter enables an increased feasible voltage range. The relevant hardware parameters are listed in Table I.

The modular structure of the hardware topology allows the device to be used in multiple EP cell configurations: In the most straightforward case, it is connected to two DC grids on either side of the DAB. Alternatively, one of the DC links may be shared with the respective AFE connected to an AC grid, thus forming an AC-DC converter with galvanic isolation. If the second DC link is also fed by the second AFE connected to another AC grid, the obtained overall structure is that of an AC-DC-AC converter with galvanic isolation, forming the topology of a solid-state transformer [5].

C. Control Structure

A variable control architecture of the EP device is required, such that each module may control either its power exchange with the grid or the grid voltage according to the electric role

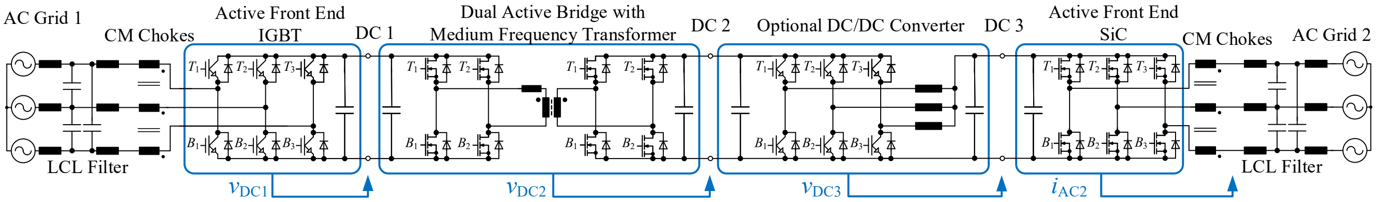

Fig. 6. Hardware topology of the realized energy packet device with example control objectives of individual PEBBs

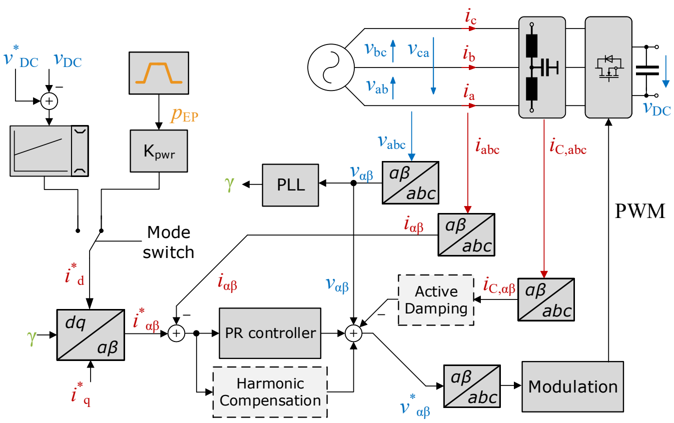

Fig. 7. AFE control structure with DC link regulation or EP power setpoint in the AC grid following case

of the participant in the connected DC or AC EP cell. To this end, both the AFEs and the DAB can be operated in a grid-forming mode, regulating the AC or DC voltage, or a grid-following mode, controlling their currents as required by its power references. Internally, the voltage of the shared DC links not connected to a DC grid also need to be controlled by one of the bordering modules. An example control configuration of the overall EP device is indicated in blue in Fig. 6, in which the EP device may act as a current controller in the AC grid 2.

Fig. 7 shows the control structure of an AFE connected to an existing AC grid. The main control objective of the AFE can either be the regulation of its DC link voltage v_{DC} or a power exchange p_{EP} with the AC grid according to an accepted EP packet transfer. DC link regulation is performed by a PI controller in the rotating dq-reference frame. In the EP-controlled mode, the currents required for the instantaneous power specified by an accepted energy packet are determined using the measured grid voltage using (1) with v_{LL} and i_{L} denoting the RMS line-to-line grid voltage and phase current.

$$p_{\mathrm{EP}} = \sqrt{3}\, v_{\mathrm{LL}}\, i_{\mathrm{L}} \cos\varphi = \sqrt{3}\, v_{\mathrm{LL}}\, \frac{i_{\mathrm{d}}}{\sqrt{2}}$$
$$\rightarrow i_{\mathrm{d}} = \sqrt{\frac{2}{3}}\, \frac{p_{\mathrm{EP}}}{v_{\mathrm{LL}}} = K_{\mathrm{pwr}}\, p_{\mathrm{EP}} \tag{1}$$

The reactive current component i_{q}^* is not used in either operating mode and can be chosen to compensate reactive power demands in the AC grid, e.g. for the connected LCL filter. The resulting currents are transformed into the stationary $\alpha\beta$-coordinate system by means of a synchronous reference frame phase-locked loop (SRF-PLL) synchronized to the grid. The requested $\alpha\beta$-current setpoints are then controlled by dampened proportional-resonant (PR) controllers described by (2), where K_{p} is the proportional gain, K_{i} the resonant gain, ω_0 the grid frequency and ω_{c} the damping coefficient. Additionally, parallel resonant paths described by (3) allow compensation of undesired harmonic current content at h multiples of the fundamental frequency:

$$G_{\mathrm{PR}}(s) = K_{\mathrm{p}} + \frac{2K_{\mathrm{i}}s}{s^2 + 2\omega_{\mathrm{c}}s + \omega_0} \tag{2}$$

$$G_{\mathrm{HC}}(s) = \sum_{h=7,11,13,17} \frac{2K_{\mathrm{ih}}\omega_{\mathrm{ch}}s}{s^2 + 2\omega_{\mathrm{ch}}s + (h\omega_0)^2} \tag{3}$$

Since the LCL grid filter may result in instabilities when not taken into account in the controller design, an active damping term based on the measured capacitor currents is also included in the current control loop.

The AC grid following control shown in Fig. 7 can be used to transfer energy packets on either the DC or AC side of the AFE. The control structure can also perform the task of the voltage controller within a DC EP cell by selecting the DC voltage v_{DC} as the control objective. If the EP device operates as a voltage controller in an AC EP cell, the control structure discussed above is not suitable. Instead, the EP device needs to act as a grid-forming converter with a different control design.

The realized EP participant with its signal processing elements and power electronic hardware is shown in Fig. 8. The flexible wiring and control concept of the EP device allows it to assume all roles required in an EP grid. With one of the AC terminals connected to the laboratory grid and the second AC terminal or one of the DC links connected to the EP cell, the device is able to emulate any EP device behavior under investigation such as PV infeed, storage services and EV charging. Alternatively, with multiple of its interfaces connected to AC or DC EP cells, the device may also act as an EP router linking those EP cells.

IV. Experimental Verification

In this section, we present experimental results of EP transfers between two realized participants. The setup for this is shown in Fig. 9a. Two of the introduced EP devices are connected together using their DC terminals in order to form an elementary EP cell. Within this DC EP cell, the DAB of the first EP device assumes the role of the voltage controller, while

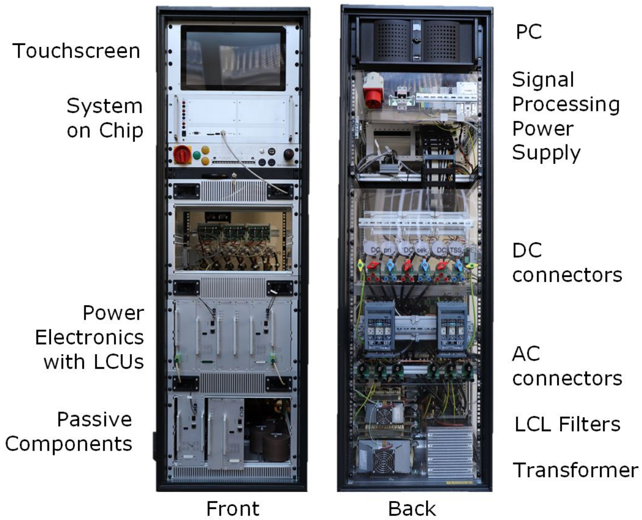

Fig. 8. Realized EP participant

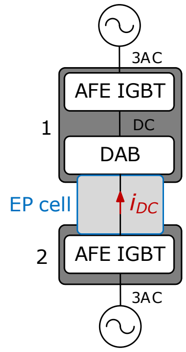

(a) Voltage and current controller

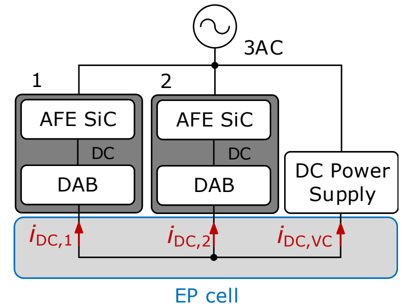

(b) Two current controllers

Fig. 9. Experiment setups with DC EP cell

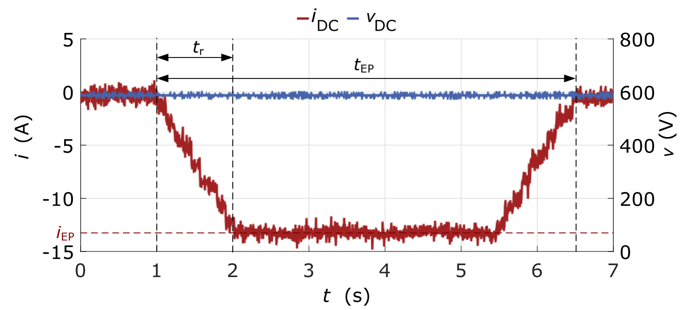

Fig. 10. Measurement of an energy packet exchange in a DC EP cell with setup shown in Fig. 9a

the IGBT AFE of the second EP device operates in a current-controlled mode. Both participants have their AC terminals connected to the laboratory AC grid, which functions as the power supply for the transmitted energy packets.

The SEPT applications running on the PCs of the participants negotiate an EP transfer. The first participant acting as the DC voltage controller also serves as the Line Manager. Line reservation, energy packet requests and acceptance messages are therefore all exchanged between the two EP devices within the laboratory network. When the packet is agreed upon, the second EP device acting as a current controller starts ramping its power conversion from the DC EP cell into the laboratory AC grid as specified by the SEPT application, shown in Fig. 10. The first EP device tasked with regulating the DC voltage consequently supplies the same amount of power in order to maintain a balance in the DC EP cell. In the depicted case, the DC grid voltage is regulated to $v_{\mathrm{DC}} = 600\,\mathrm{V}$. The negotiated EP transfer specifies a total energy of $W_{\mathrm{EP}} = 36\,\mathrm{kJ}$ with a defined power of $P_{\mathrm{EP}} = 8\,\mathrm{kW}$ and ramping phases chosen as $t_{\mathrm{r}} = 1\,\mathrm{s}$. This results in a steady-state DC current of $i_{\mathrm{EP}} = \frac{8\,\mathrm{kW}}{600\,\mathrm{V}} = 13.3\,\mathrm{A}$ and a packet duration of $t_{\mathrm{EP}} = \frac{36\,\mathrm{kJ} - 8\,\mathrm{kW}\cdot 1\,\mathrm{s}}{8\,\mathrm{kW}} + 2\,\mathrm{s} = 5.5\,\mathrm{s}$.

The two realized EP devices can also both assume the role of current controllers in the DC EP cell. With only two EP devices available, the DC voltage needs to be regulated by an additional power supply with a setpoint of $v_{\mathrm{DC}} = 600\,\mathrm{V}$. The experiment setup for this configuration is shown in Fig. 9b. Both EP devices and the DC power supply are connected to the laboratory AC grid in order to inject or consume the requested power into the DC EP cell. With their DC terminals, all three devices are connected to the same DC EP cell. In both EP devices, the DABs perform a galvanically isolated DC/DC conversion and regulate the voltage of the DC links connecting them to the SiC AFE within the same EP device. The AFEs can therefore control their power exchange with the AC grid using the DC link as its energy source. The power exchange is controlled to follow the power curve determined using a SEPT negotiation. This behavior is shown in the measurement in Fig. 11. The current offsets visible at $t = 0$ and after the EP transfer finishes are caused by losses and the passive discharging resistors in the EP devices that are supplied by the DC power supply. After the two EP devices agree on an EP transfer, they both start ramping their DC currents i_1 and i_2 in opposite directions according to the EP power curve. In this scenario, there is no visible communication latency that would result in a compensation current i_{VC}. The negotiated EP transfer specifies a total energy of $W_{\mathrm{EP}} = 20\,\mathrm{kJ}$ with a stationary power of $P_{\mathrm{EP}} = 5\,\mathrm{kW}$ and ramping phases lasting $t_{\mathrm{r}} = 1.67\,\mathrm{s}$. This results in a steady-state DC current of $i_{\mathrm{EP}} = \frac{5\,\mathrm{kW}}{600\,\mathrm{V}} = 8.33\,\mathrm{A}$ and a packet duration of $t_{\mathrm{EP}} = \frac{20\,\mathrm{kJ} - 5\,\mathrm{kW}\cdot 1.67\,\mathrm{s}}{5\,\mathrm{kW}} + 3.33\,\mathrm{s} = 5.67\,\mathrm{s}$.

Another EP exchange with the same energy content, but higher power and faster ramping is shown in Fig. 12. In this case, the EP parameters are set to $W_{\mathrm{EP}} = 20\,\mathrm{kJ}$, $P_{\mathrm{EP}} = 6\,\mathrm{kW}$, $t_{\mathrm{r}} = 0.5\,\mathrm{s}$. With a higher peak power and shorter ramping phases, the packet duration is now $t_{\mathrm{EP}} = \frac{20\,\mathrm{kJ} - 6\,\mathrm{kW}\cdot 0.5\,\mathrm{s}}{6\,\mathrm{kW}} + 1\,\mathrm{s} = 3.83\,\mathrm{s}$.

V. Conclusion

The present paper proposes a hardware realization of a flexible EP device for laboratory experiments. We introduce the design of a flexible power electronics topology valid for

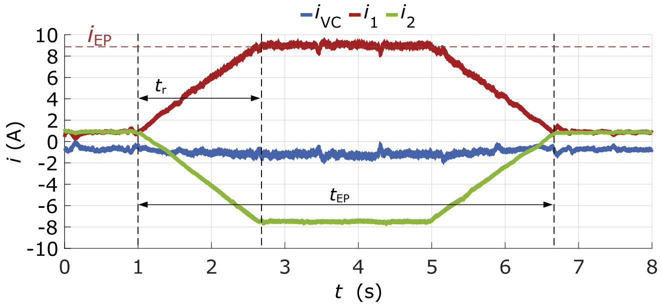

Fig. 11. Measurement of an energy packet exchange between two current-controlled EP devices with setup in Fig. 9b

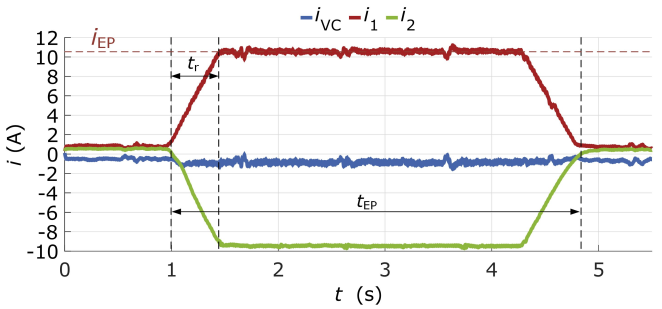

Fig. 12. Measurement of an energy packet with higher power and faster ramping with setup in Fig. 9b

all EP cell configurations and show the signal processing and control structures required for an EP-based grid operation. The feasibility of the described concept is proven with experimental validation of basic EP transfers, both between voltage- and current-controlled EP devices and between two current-controlled EP devices.

Future work includes the operation of the EP device in a AC grid forming mode, the application of the shown EP device realization as an EP router and an EP cell with multiple participants and parallel voltage controllers.

References

[1] J. A. P. Lopes, N. Hatziargyriou, J. Mutale, P. Djapic, and N. Jenkins, "Integrating distributed generation into electric power systems: A review of drivers, challenges and opportunities," *Electric Power Systems Research*, vol. 77, no. 9, pp. 1189–1203, Jul. 2007.

[2] E. J. Coster, J. M. A. Myrzik, B. Kruimer, and W. L. Kling, "Integration Issues of Distributed Generation in Distribution Grids," *Proceedings of the IEEE*, vol. 99, no. 1, pp. 28–39, Jan. 2011.

[3] R. Gupta, A. Pena-Bello, K. N. Streicher, C. Roduner, Y. Farhat, D. Thöni, M. K. Patel, and D. Parra, "Spatial analysis of distribution grid capacity and costs to enable massive deployment of PV, electric mobility and electric heating," *Applied Energy*, vol. 287, Apr. 2021.

[4] N. Hatziargyriou, Ed., *Microgrid: architectures and control*. Chichester, West Sussex, United Kingdom: Wiley, 2013.

[5] M. Liserre, G. Buticchi, M. Andresen, G. De Carne, L. F. Costa, and Z.-X. Zou, "The Smart Transformer: Impact on the Electric Grid and Technology Challenges," *IEEE Industrial Electronics Magazine*, vol. 10, no. 2, pp. 46–58, Jun. 2016.

[6] S. Kampezidou, O. Vasios, and S. Meliopoulos, "Multi-Microgrid Architecture: Optimal Operation and Control," in *2018 North American Power Symposium (NAPS)*. Fargo, ND: IEEE, Sep. 2018, pp. 1–5.

[7] G. Kariniotakis, L. Martini, C. Caerts, H. Brunner, and N. Retiere, "Challenges, innovative architectures and control strategies for future networks: the Web-of-Cells, fractal grids and other concepts," *CIRED - Open Access Proceedings Journal*, vol. 2017, pp. 2149–2152, Oct. 2017.

[8] J. Toyoda and H. Saitoh, "Proposal of an open-electric-energy-network (OEEN) to realize cooperative operations of IOU and IPP," in *Proceedings of EMPD '98. 1998 International Conference on Energy Management and Power Delivery (Cat. No.98EX137)*, vol. 1, Mar. 1998, pp. 218–222 vol.1.

[9] R. Takahashi, K. Tashiro, and T. Hikihara, "Router for Power Packet Distribution Network: Design and Experimental Verification," *IEEE Transactions on Smart Grid*, vol. 6, no. 2, pp. 618–626, Mar. 2015.

[10] K. A. Corzine, "Energy packets enabling the energy internet," in *2014 Clemson University Power Systems Conference*, Mar. 2014, pp. 1–5.

[11] R. Rojas-Cessa, C. Wong, Z. Jiang, H. Shah, H. Grebel, and A. Mohamed, "An Energy Packet Switch for Digital Power Grids," in *2018 IEEE International Conference on Internet of Things (iThings) and IEEE Green Computing and Communications (GreenCom) and IEEE Cyber, Physical and Social Computing (CPSCom) and IEEE Smart Data (SmartData)*, Jul. 2018, pp. 146–153.

[12] M. M. He, E. M. Reutzel, X. Jiang, R. H. Katz, S. R. Sanders, D. E. Culler, and K. Lutz, "An Architecture for Local Energy Generation, Distribution, and Sharing," in *2008 IEEE Energy 2030 Conference*, Nov. 2008, pp. 1–6.

[13] R. Abe, H. Taoka, and D. McQuilkin, "Digital Grid: Communicative Electrical Grids of the Future," *IEEE Transactions on Smart Grid*, vol. 2, no. 2, pp. 399–410, Jun. 2011.

[14] P. H. J. Nardelli, H. Alves, A. Pinomaa, S. Wahid, M. D. C. Tomé, A. Kosonen, F. Kühnlenz, A. Pouttu, and D. Carrillo, "Energy Internet via Packetized Management: Enabling Technologies and Deployment Challenges," *IEEE Access*, vol. 7, pp. 16 909–16 924, 2019.

[15] I. Kouveliotis-Lysikatos, N. Hatziargyriou, Y. Liu, and F. Wu, "Towards an Internet-Like Power Grid," *Journal of Modern Power Systems and Clean Energy*, pp. 1–11, 2020.

[16] K. Wang, J. Yu, Y. Yu, Y. Qian, D. Zeng, S. Guo, Y. Xiang, and J. Wu, "A Survey on Energy Internet: Architecture, Approach, and Emerging Technologies," *IEEE Systems Journal*, vol. 12, no. 3, pp. 2403–2416, Sep. 2018.

[17] D. Boroyevich, I. Cvetkovic, R. Burgos, and D. Dong, "Intergrid: A Future Electronic Energy Network?" *IEEE Journal of Emerging and Selected Topics in Power Electronics*, vol. 1, no. 3, pp. 127–138, Sep. 2013.

[18] S. Keshav and C. Rosenberg, "How internet concepts and technologies can help green and smarten the electrical grid," in *Proceedings of the first ACM SIGCOMM workshop on Green networking*. New York, NY, USA: Association for Computing Machinery, Aug. 2010, pp. 35–40.

[19] A. Monti, E. De Din, D. Müller, F. Ponci, and V. Hagenmeyer, "Towards a real digital power system: An energy packet approach," in *2017 IEEE Conference on Energy Internet and Energy System Integration (EI2)*, Nov. 2017, pp. 1–6.

[20] B. Zhang and J. Baillieul, "A packetized direct load control mechanism for demand side management," in *2012 IEEE 51st IEEE Conference on Decision and Control (CDC)*, Dec. 2012, pp. 3658–3665.

[21] P. Rezaei, J. Frolik, and P. D. H. Hines, "Packetized Plug-In Electric Vehicle Charge Management," *IEEE Transactions on Smart Grid*, vol. 5, no. 2, pp. 642–650, Mar. 2014.

[22] M. Almassalkhi, L. D. Espinosa, P. D. H. Hines, J. Frolik, S. Paudyal, and M. Amini, *Asynchronous Coordination of Distributed Energy Resources with Packetized Energy Management*. New York, NY: Springer, 2018.

[23] L. A. D. Espinosa, A. Khurram, and M. Almassalkhi, "Reference-Tracking Control Policies for Packetized Coordination of Heterogeneous DER Populations," *IEEE Transactions on Control Systems Technology*, vol. 29, no. 6, pp. 2427–2443, Nov. 2021.

[24] K. Schneider, F. Wiegel, D. Schulz, V. Hagenmeyer, M. Hiller, R. Bless, and M. Zitterbart, "Designing the Interplay of Energy Plane and Communication Plane in the Energy Packet Grid," in *2021 IEEE 46th Conference on Local Computer Networks (LCN)*, Oct. 2021, pp. 331–334.

[25] B. Schmitz-Rode, L. Stefanski, R. Schwendemann, S. Decker, S. Mersche, P. Kiehnle, P. Himmelmann, A. Liske, and M. Hiller, "A modular signal processing platform for grid and motor control, hil and phil applications," in *2022 International Power Electronics Conference (IPEC)*, 2022, preprint.